THE OXIDATION KINETICS OF ZIRCONIUM AT 800° AND 850°C.

by

HAMIDUZZAMAN AKRAM KAZI, B.Sc.

A Thesis

Submitted to the Faculty of Graduate Studies

in Partial Fulfilment of the Requirements

for the Degree

Master of Engineering

McMaster University

May, 1963

TABLE OF CONTENTS

LIST OF ILLUSTRATIONS

LIST OF TABLES

CHAPTER I

INTRODUCTION

Due to the technological developments in different fields, like rocket and atomic reactor engineering, use of some less abundant metals at high temperatures has become very important. Zirconium is one of the important metals for reactor use. This thesis is concerned with an investigation of the oxidation kinetics of zirconium at high temperatures.

The mechanisms for oxidation of metals has been surveyed by Evans (1), Kubaschewski and Hopkins (2) and many other investigators. From the theoretical considerations of oxidation phenomena Wagner (3) developed a mathematical theory for "parabolic oxidation" in 1933. Later, Cabrera and Mott (4) published a theory which explains a number of relationships for the rate of growth of oxide scales. Evans (1) pointed out the existance of stress in oxide films and suggested an alternative formulation for the parabolic rate law. These theories have been expanded by others, and many detailed experiments have been based on them.

Despite the considerable number of investigations that have been carried out on different metals and alloys, the general characteristics of oxidation are not yet clear, and further detailed studies of the mechanisms involved are required. In this thesis, we are dealing with the oxidation of metals in Periodic Subgroup IVB, titanium, zirconium

and hafnium. These metals follow very similar rate equations which can be attributed to the diffusion of oxygen in superficial dioxide films and scales (5-9). At intermediate temperatures, the kinetics follow logarithmic, cubic and parabolic equations in order of increasing exposure while, at high temperatures, the kinetics follow a parabolic-linear equation.

From common knowledge we know that most metals possess an "affinity" for oxygen; that is, the combination of oxygen and atmospheric pressure with almost all metals (except possibly a few noble metals such as gold) results in a drop of free energy - so that the reaction is capable of occurring spontaneously. Thus the production of an oxide on the surface of a metal exposed to oxygen tends to isolate the metal from oxygen. The oxide film then can only grow by the movement of metal ions outward or oxygen inwards. Such movement is possible, in cases where the oxide contains interstitial metal or vacant lattice sites.

Smeltzer, Haering and Kirkaldy (10) have constructed a phenomenological theory to account functionally for the kinetics of oxidation at intermediate temperatures. It was based on the model that oxygen migrates through the oxide lattice and through low resistance paths of temporerily decreasing effectiveness under the influence of the oxygen gradient. The equation involves three parameters: the parabolic rate constant, the ratio of the diffusion constants for short circuit and lattice diffusion and the fraction of available oxygen sites lying within low resistance paths. The latter were assumed to decay in time as a first order rate process. Those kinetics previously represented in temporal order by logarithmic, cubic and parabolic equations were represented in this theory

by a single exponential relation. It was demonstrated that this equation adequately represents the oxidation kinetics of titanium, zirconium and hafnium in the temperature range 300°-600°C.

Parabolic oxidation is associated with the development of a compact scale and concurrent penetration of oxygen into the metal substrate. The change of parabolic to linear kinetics is brought about by complete or partial breakdown of compact oxide whereupon the oxygen distribution in the metal attains a steady configuration in a reference system moving with the oxide/metal interface (8). It has been reported for titanium that the scale becomes a completely porous envelope by compression mechanisms involving either exfoliation, blistering or cracking of the compact oxide at critical thicknesses or critical metallic oxygen contents (8, 11, 12). On the other hand, the transitions to linear oxidation kinetics for zirconium and hafnium appear to be brought about by formation of duplex scale consisting of adjacent porous and compact oxide layers (13, 9). Consequently, linear kinetics for these metals are probably controlled by the inward diffusion rate of oxygen through the remnant compact oxide layers.

To the present, it has not been demonstrated that the transition from parabolic to linear oxidation for zirconium is associated with the formation of a duplex scale. Results are reported here which confirm the viewpoint of duplex scale formation where the scale consists of a compact inner layer overlain by a porous outer oxide layer. This porous outer layer provides no resistance to the direct contact of oxygen with the compact inner layer. Also, an oxide-metal diffusion model is advanced to account for the kinetics of oxidation. Our experimental observations confirm the validity of the diffusion model.

CHAPTER II

LITERATURE REVIEW

2.1 Introduction

If a metal or alloy is brought in contact with oxygen, and if the thermodynamic conditions for a reaction are favourable, one can observe a more or less rapid reaction in which the reaction products appear as a surface layer. The mechanism and rate of surface layer formation vary depending upon experimental conditions. A very thin surface layer formed on a metal during oxidation is generally compact, adherent and pore free. This is also observed if the reaction-product layer is of smaller molar volume than the atomic volume of the metallic phase, although the Pilling and Bedworth's rule (14) states that compact surface layer can only be expected if the ratio of molar volume of surface layer to metal is greater than one.

In the case of metal oxidation by gaseous oxygen, the nature and extent of particle transport depend upon the defect model of oxide constituting the surface layer. For example, in the case of zinc oxidation the zinc oxide surface layer contains zinc ions in interstitial lattice sites. Consequently, zinc ions migrate through interstitial lattice sites together with free electrons towards the outer ZnO boundary. In case of copper oxidation to cuprous oxide, where copper ion vacancies and electron holes are formed due to a metal deficiency, outward migration of Cu ions and electrons takes place through vacancies and holes.

between electron defects, the number of which is equivalent to the number of ion defects in the lattice. However, the slower transport rate of ions is generally the rate determining step in an oxidation reaction. Thus, a concentration gradient of ions is established and the oxidation rate is controlled by the diffusion rate of metallic or oxygen ions through the superficial oxide layer.

A useful approximation to the equation for parabolic oxidation may be derived as follows. Assuming that an electrical field does not exist across the oxide film, the ion current is,

$$J = -D \frac{dc}{dx} \qquad (1)$$

where D is the diffusion coefficient and $\frac{dc}{dx}$ is the concentration gradient of interstitial ions, cation or anion vacancies. Thus the rate of film growth is,

$$\frac{dx}{dt} = J\Omega = -D \frac{dc}{dx} \qquad (2)$$

if Ω is the volume of oxide per ion. Since the concentration gradient is inversely proportional to the film thickness, integration gives the equation of the parabolic law,

$$x^2 = k_1 t + k_2$$

where $k_1 = 2D (n_1 - n_2)$ and $k_2 = 0$

Here, n_1 and n_2 are the numbers of interstitial ions or vacancies per cubic centimeter at the oxide/oxygen and oxide/metal interfaces.

There have been many variations and developments of this basic theory as pointed out by Kubaschewski and Hopkins (17). The significance of these equations is not that they provide a method of predicting oxidation rates but if the rate equations agree with experimental

results, the underlying assumptions concerning the oxidation mechanism may be supported.

2.2 (b) CABRERA AND MOTT THEORY

Cabrera and Mott (4) have presented a theory of oxidation to explain each of the various rate equations, and in order to do so, divided the scales into three thickness ranges; thick scales, films, and very thin films. For thick scales in which electronic neutrality may be maintained, they developed expressions for the parabolic oxidation of metals forming metal-deficit and metal-excess oxide scales. It is generally considered that their main contribution was made in the field of very thin films, (100Å or less). They postulated that the oxide film may behave as an electrical dipole layer due to the rapid transport of electrons across the film to form oxygen ions from adsorbed oxygen. The velocity of the drift of the ions then becomes dependent upon the electrical field strength and metallic ions escaping from the metal surface may, in fact, be directly pulled across the film to react at the oxide/oxygen interface. This type of oxide growth may exist only up to a limiting film thickness. Reactions of this type follow an inverse logarithmic law of oxidation and many metals oxidize at room temperature by this relationship.

2.3 Oxidation in General for Subgroup IVB Metals

Titanium and hafnium, like zirconium, exhibit unusually high solubilities for oxygen. These metals of Periodic Subgroup IVB possess similar chemical characteristics. In this literature review, titanium and hafnium will be considered with zirconium in order to correlate their similar oxidation characteristic and also to facilitate clearer understanding of zirconium oxidation.

2.4 Oxidation of Titanium

Fast (18) in 1938 and Ehrlich (19) in 1941 found that oxygen forms a solid solution with titanium beneath the oxide scale. In 1949 Gulbransen and Andrew (20) showed that after an "initial period" the oxidation reaction in the temperature range 250°-600°C for the period of two hours followed a parabolic growth equation.

Alexander and Pidgeon (21) concluded from their oxidation experiments over the temperature range 250°-550°C, that two mechanisms are involved in the oxidation process:

(a) The formation of their film.

(b) The solution of oxygen in the metal.

Below 300°C the first mechanism is predominant and oxygen absorption is limited. The reaction in this case followed a logarithmic growth equation. Above 450°C the oxidation of titanium involved solution of oxygen in the metal by a diffusion controlled process, and again a logarithmic equation best fitted their results.

In 1953 Waber, Sturdy and Wise (22) confirmed the investigation of Alexander and Pidgeon. They suggested that the break in Arrhenius plot reported by Gulbransen and Andrew (20), at 350°C was due to a change from the logarithmic to the parabolic equation.

Jenkins (23) then showed that for titanium the oxide formation occurs at the scale/metal interface. The scales formed in the temperature range 600°-925°C were porous. He established the oxygen gradient in the metal by microhardness measurements and from these results suggested a mechanism for the oxidation of titanium at high temperatures. Oxygen diffused into the metal core but the oxidation rate was controlled by

diffusion in the scale. He also suggested that the transformation of the initial parabolic to linear growth occurs when the thickness of scale is built up to a thickness beyond which it can not exist without rupture.

Examination of the oxidation of saturated and unsaturated titanium specimens in the temperature range 800°-1200°C by Simnad, Spilners and Katz (24) has shown that initial oxidation rates were parabolic irrespective of the oxygen content of the metal. The parabolic rates, however, were lower for the specimens saturated with oxygen.

In further study of the oxidation of titanium, using an accurate volumetric method, Jenkins (25) checked the kinetic reaction obtained between 650° and 950°C. He found that the parabolic growth changed abruptly to a linear growth at decreasing time with increasing temperature. Further abrupt changes were found to occur at irregular intervals after long oxidizing times. In discussing his results, Jenkins, using an analytical method put forward by Wagner, showed that reaction at either the gas/scale interface or the scale/metal interface were unlikely to be controlled reactions. Therefore, the rate of diffusion of oxygen in the scale and metal core was assumed to control the oxidation rate.

Kinna and Knorr (26) suggested for their experimental results carried at 800°, 1000° and 1200°C that at the beginning of oxidation rutile is formed, through which titanium ions diffuse outwards and oxygen ions diffuse inwards, forming a titanium-oxygen solid solution in the core. After several hours, the outer layer of rutile becomes dense and on its under surface a layer of porous oxide forms.

Kofstad, Hauffe, and Kjollesdale (27) found four different growth equations from their investigations; logarithmic below 300°C, cubic from 300°C to 600°C, parabolic from 600°C to 850°C, and parabolic and linear above 850°C. The initial growth equation observed at any temperature eventually changed into a growth equation corresponding to the higher temperature level. They assumed that the diffusion of oxygen ions through the scale was the rate determining step-below 1000°C, and suggested that the logarithmic growth equation resulted from an oxide film formation, governed perhaps, by a Mott type mechanism. The cubic growth equation was assumed to be associated with the diffusion of oxygen into the metal core and the parabolic growth equation was interpreted in terms of the usual Wagner high temperature mechanism. Linear growth resulted when cracks were found due to stresses in the oxide scale and, at this stage of oxidation, a phase boundary reaction became the rate determining reaction.

Wallwork, G. R., (28) has concluded from his study of the oxidation of titanium at high temperature that oxygen dissolves in the metal lattice to form a gradient beneath the scale. The oxidation process is governed by the movement of this gradient, and growth may be parabolic and linear, consecutively, for high temperatures of oxidation. The establishment of a "steady gradient" coincided with the transition of the growth equation from a parabolic to linear oxidation. In his experiments he could not establish that linear growth was controlled by diffusion in the oxide scale. He also found that the oxide had seven percent porosity and that oxidation of a specimen saturated with oxygen was linear instead of parabolic as expected. He suggested more accurate work

to establish that linear oxidation is associated with the diffusion process in the metal.

The oxidation of titanium in the temperature range 850°-1000°C has been recently investigated by Stringer (11). The initial parabolic rate was superseded by a second parabolic rate, considerably more rapid than the first. In general, the lower the temperature, the longer before the first parabolic rate law broke down. He determined the partition of oxygen between the scale-forming and oxygen solution reactions. The proportion of oxygen entering the metal remained constant at about 45 percent during the first parabolic section. As the relative amounts of oxygen in the metal and scale remained constant during the initial parabolic stage, both the formation of scale and solution of oxygen separately must be parabolic. After the break-away the proportion dropped until by the time the second parabola was established only about 5 percent of the total oxygen absorbed was present in the metal. For this stage of oxidation, the most probable step for the control of the kinetic appeared to be gaseous diffusion of oxygen through the porous scale.

2.5 Oxidation of Hafnium

Very little information has been published about the oxidation of hafnium. Smeltzer and Simnad (9) investigated the oxidation kinetics in the temperature range 350°-1200°C. Although information is not available on the solubility of oxygen in hafnium, they noted that oxygen dissolved in the metal phase beneath scales on oxidized specimens. The kinetics followed the parabolic relationship in the temperature range 350°-800°C after an initial deviation. In this early stage of oxidation, the kinetics would be represented by a logarithmic equation. Thus the

rate of scale growth in the temperature range 350°-800°C followed a logarithmic plus parabolic equation for the investigated exposure periods. Between 900 and 1200°C, the growth equations were parabolic after an initial deviation and became linear during long periods of oxidation. Although they were unable to measure the weight increases in the early stages of oxidation, the authors suggested that in their temperature range the initial period might also be described by a logarithmic equation. In interpreting their results, the authors suggested that the rate controlling process was the diffusion of oxygen through the scale, and that a linear growth equation was obtained when porous oxide formed over a compact layer which had grown to a maximum thickness. X-ray diffraction showed that the scale was monoclinic hafnia. Utilizing radio-active markers, scale growth was shown to occur by the inward diffusion of oxygen.

Wallwork and Jenkins (8) have studied several features of the parabolic-linear oxidation kinetics of hafnium. They established the formation of a duplex scale. Adherent compact gray oxide was formed below porous oxide and establishment of the steady oxygen gradient in the metal coincided with the change from a parabolic to a linear growth equation.

2.6 Oxidation of Zirconium

According to Cubicio (29, 30) the zirconium dissolves larger amounts of oxygen than titanium, Lintton (31) established that oxygen penetrated into the metal during oxidation. The effect of oxygen additions on the lattice constants of zirconium was investigated by Treco (32). He found

that the lattice expanded linearly with increasing amount of oxygen. Also, the hardness of zirconium was increased in direct proportion to the increasing amounts of dissolved oxygen.

Hayes and Roberson (33, 34) found, in 1948-49, that on heating zirconium in air in the temperature range 425 to 1300°C, a marked increase in the oxidation rate occurred near 900°C. In 1949, Gulbransen and Andrew (35), using a microbalance, determined the growth equation for the oxidation of "abraded" samples in pure oxygen in the temperature range 200°-435°C for periods of 120 minutes. Their results were best fitted to a parabolic growth equation. In 1951, Cubiciott (30) investigated the temperature range 600°-900°C and found that a parabolic rate equation was followed for periods up to two hours but noted that a small deviation towards a linear relationship occurred at 920°C in this period. In the same year Phalnikar and Baldwin (36) reported a parabolic oxidation relationship for zirconium heated in air until a white scale formed. They reported an enormous increased rate when white scale appeared. Belle and Mallet (37) reported in 1954, however, that in the temperature range 575°-950°C the results were best fitted to a cubic equation. Charles, Barnatt and Gulbransen (38) also showed that in the temperature range 350°C and 450°C for the periods of 400 hours the results were fitted to a cubic equation. Kendall (39) found that for prolonged periods of exposure in the temperature range of 500°-700°C the parabolic oxidation changes to linear.

As shown by Belle and Mallet (37) specimens oxidized at 575°C do not exhibit oxygen penetration in the metal phase. At the higher temperature of 875°C oxygen did penetrate into the metal phase.

In 1959, Wallwork (28) studied the high temperature oxidation properties of zirconium and found the following facts. Strongly adherent gray compact oxides with some visable porosity were formed with white ridges showing the edges. Gray scales, when stripped from the metal and heated in oxygen, turned white. There were no layering in the scale structure. Both the white and gray forms of scale were shown by x-ray diffraction to be monoclinic. The oxidation kinetics at 850°C followed a parabolic plus linear rate equation with the change occurring in the vicinity of 24 hours. The oxygen penetration reached a "steady gradient" after 24 hours. Thus the establishment of the steady gradient coincided with the change from the parabolic to linear relationship. He concluded that the scale was non-protective and that the oxidation process was controlled by the interstititial diffusion of oxygen in the metal phase.

In 1961, Cox (40) discussed the mechanism of oxide film growth and breakdown on zirconium. He has suggested that, in the initial period at least, two mechanisms of film growth are operating simultaneously, and after breakaway there is indefinite linear growth. From the nature of the breakaway process at high temperature, he has suggested that at a critical film thickness, cracking of the film occurs due to stresses set up in it during growth. These stresses may result from the high Pilling-Bedworth ratio of 1.56.

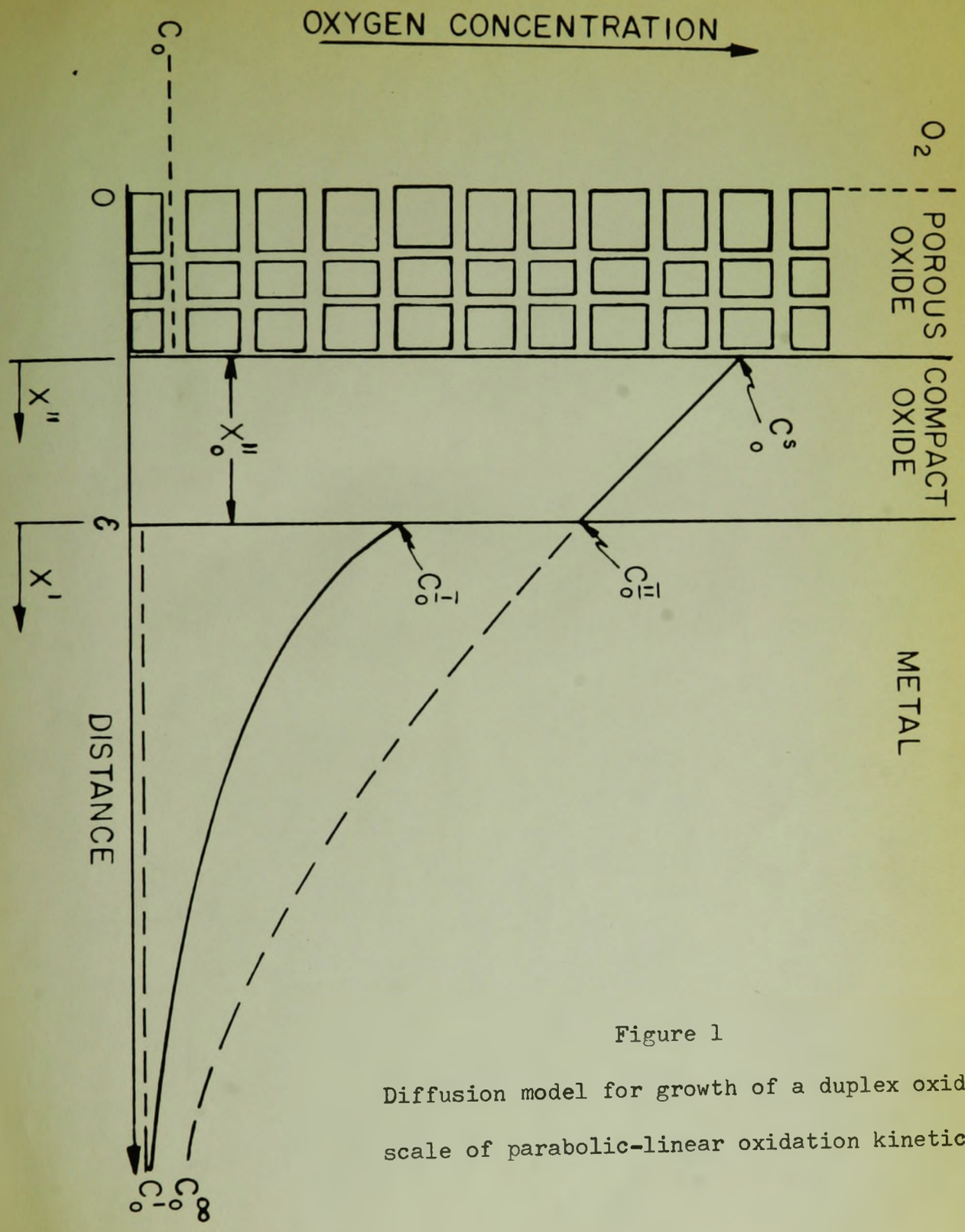

Figure 1

Diffusion model for growth of a duplex oxide scale of parabolic-linear oxidation kinetics.

of oxygen in the metal corresponds to a model advanced by Wagner (41) for diffusion in a two-phase system. He has demonstrated that diffusion theory in terms of constants D_o^I and D_o^{II} for metal and oxide, respectively, lead to a parabolic growth law. It will be demonstrated subsequently that the oxygen uptake of metal amounts to only from 15 to 30 percent of the total in the temperature range 800°-850°C. Accordingly, it is assumed that a constant oxygen gradient in the oxide serves as a good first approximation to obtain the low gradient expression for the parabolic growth law of compact oxide,

$$x^2 = k_p^{II} t \qquad (1)$$

where $$k_p^{II} = 2\Omega D_o^{II} (C_o^s - C_o^{II}) \qquad (2)$$

Here, Ω is the volume of oxide per g oxygen ion and C_o^s and C_o^{II} are the oxygen concentrations (g/cc) in the oxide/oxygen and oxide/metal interfaces, respectively.

From the model it is possible to evaluate the parameters for linear oxidation. During this stage of porous oxide formation, the metal interface and oxygen profile in the metal move inward at a constant rate. Thus an extension of the analyses carried out by Tiller et al (42) and Wagner (43) for diffusion in a phase where the boundary migrates at a constant rate may be applied. With the help of Fick's law, $J_x = -D(\frac{dc}{\partial x})_x$ or $J_{x+dx} = -D(\frac{dc}{\partial x})_{x+dx}$ the net flow in the volume element, from Tiller's formula is $D(\frac{d^2c}{dx^2})$ per unit volume. If K_L is the linear rate constant in cm/sec, the total flow out is $K_L(\frac{dc}{dx})$. Then the diffusion equation for a steady state concentration distribution in a system moving at a velocity K_L is,

$$D\frac{d^2c}{dx^2} + K_L\left(\frac{dc}{dx}\right) = 0 \quad \text{or} \quad \frac{d^2c}{dx^2} + \frac{K_L}{D}\frac{dc}{dx} = 0 \qquad (3)$$

The solution for this equation can be obtained by putting $c = e^{mx}$

$$\frac{dc}{dx} = me^{mx} \qquad (i)$$

$$\frac{d^2c}{dx^2} = m^2e^{mx} \qquad (ii)$$

Putting values (i) and (ii) in (3)

$$Dm^2 + Rm = 0 \qquad (iii)$$

or $m(Dm + R) = 0$

$$m = 0 \qquad (iv)$$

$$m = -\frac{K_L}{D} \qquad (v)$$

$$C = A.\ e^{-K_L/D\ x} + B$$

When $x = \alpha$, $C_o' = B$

$x = 0$, $C_o^I = A + B$

The appropriate solution for the metal phase with distance $x = x'$ measured from the oxide/metal interface is,

$$C^I(x') = (C_o^I - C_o')\exp\left(-\frac{K_L}{D_o^I}x'\right) + C_o \qquad (4)$$

and for the compact oxide phase with distance $x = x''$ measured from the oxide/gas interface if,

$$C^{II}(x'') = (C_o^s - C_o)\exp\left(-\frac{K_L}{D_o^{II}}x''\right) + C_o^\alpha \qquad (5)$$

A fit of equation (4) to the oxygen penetration curve within the metal will be used to give an estimate of D_o^I for comparison with independent values in the literature as a check on the linear growth model for the metal.

The uptake of oxygen by the metal before onset of linear oxidation may first be evaluated. This amount is therefore,

$$\left(\frac{\Delta M}{A}\right)_{metal} = \int_o^\infty C^I\,dx' - \int_o^\infty C_o'\,dx' \qquad (6)$$

$$= \int_o^\infty (C_o^I - C_o')\exp\left(-\frac{K_L}{D_o^I}x'\right)dx' + \int_o^\infty C_o'\,dx' - \int_o^\infty C_o'\,dx'$$

$$\simeq \frac{D_o^I}{K_L}(C_o^I) \qquad (7)$$

if the initial metallic concentration of oxygen (C_o') is assumed to be negligible.

As a second consideration, an expression for the parabolic constant of compact scale growth (K_p^{II}) in terms of the linear rate constant (K_L) can be evaluated. The boundary condition at the oxide/metal interface gives,

$$C_o^{II} - C_o^\alpha = (C_o^s - C_o^\infty)\exp\left(-\frac{K_L}{D_o^{II}}x_o''\right) \qquad (8)$$

while the mass balance gives,

$$(C_o^{II} - C_o^I)K_L - D_o^I\left(\frac{\partial C^I}{\partial x}\right)_{x'=o} = -D_o^{II}\left(\frac{\partial C^{II}}{\partial x''}\right)_{x''=x_o''} \qquad (9)$$

or

$$C_o^{II} - C_o' = (C_o^s - C_o^\infty)\exp\left(-\frac{K_L}{D_o^{II}}x_o''\right) \qquad (10)$$

Comparison with equation (8) shows that for a solution to exist one has to set,

$$C_o^\infty = C_o' \qquad (11)$$

There is one further condition which must be imposed on the two solutions and that is the mass balance at the oxygen/oxide interface,

$$(C_o^s - C_o)K_L = -D^{II}\left(\frac{\partial C}{dx}\right)_{x''=o} = K_L(C_o^s - C_o^\infty) = K_L(C_o^s - C_o') \qquad (12)$$

where C_o is the atmospheric oxygen concentration. Hence, for the steady solution to exist it must be that,

$$C_o = C_o' \qquad (13)$$

There was no need to achieve this condition in the experiments since both C_o and C_o' are sufficiently small to be set equal to zero, thus obtaining effective equality. For example, the oxygen concentration in an atmosphere at S.T.P. is 1.43×10^{-3} g./cc. This concentration would

correspond to a metallic impurity oxygen content of only 0.02 weight percent. Moreover, C_o^s is much larger than C_o because the oxygen concentration of stoichiometric zirconium dioxide is 1.49 gm/cc.

An expression can now be obtained for the parabolic rate constant (K_p^{II}) for compact scale growth in terms of the linear rate constant (K_L) by solving equation (5).

If the oxide phase is considered as a semi-infinite plate moving with a gradient constant with time

$$C^{II}_{(x'')} = (C_o^s - C_o) \exp\left(-\frac{K_L}{D_o^{II}} x''\right) + C_o$$

When the thickness of compact scale is maximum $x'' = x_c''$

$$C^{II}_{x_o''} = (C_o^s - C_o^\infty) \exp\left(-\frac{K_L}{D_o^{II}} x_o''\right) + C_o^\infty$$

Taking $C_o^\infty = C_o = C'$ and neglecting the value of C_o

$$\frac{C_o^{II}}{C_o^s} = \exp\left(-\frac{K_L}{D_o^{II}} x_o''\right)$$

or,

$$K_L x_o'' = D_o^{II} \ln \frac{C_o^s}{C_o^{II}} - D_o^{II} \left(\frac{C_o^s - C_o^{II}}{C_o^{II}}\right) \qquad (14)$$

or,

$$K_L x_o'' C_o^{II} = D_o^{II} (C_o^s - C_o^{II}) \qquad (15)$$

The left hand side can be evaluated empirically from the linear rate data and the phase diagram. It can be substituted into the expression for the parabolic rate constant, equation (2), to give an independent value of this parameter for comparison with the directly determined value. This serves as a check on the linear growth model for the oxide.

This analysis will be applied insofar as possible to the high

CHAPTER IV

EXPERIMENTAL APPARATUS AND METHODS

4.1 Oxidation Apparatus

A diagram of the apparatus used for the measurements of oxidation rates is illustrated in figure 2, showing the pyrex glass vacuum system, furnace and spiral spring balance arrangement.

4.1 (a) VACUUM SYSTEM

The vacuum system used was of conventional design and consisted of a mechanical pump (1), a two stage oil diffusion pump (2), oxygen storage flasks (3) and cold traps (4), placed in such a way as to protect the metal specimens from moisture, oil vapour or mercury vapour. The vacuum was measured with a McLeod gauge. The vacuum system could maintain the assembly at a pressure of 10^{-6} mm Hg.

4.1 (b) FURNACE

The furnace (5) was of simple construction. The heating element consisted of michrome wire wound around a mullite tube and then covered by a layer of refractory paste. This furnace was capable of operating at 1000°C for long periods of time. The hot spot of the furnace was about two inches in length and about 6 inches below the top of the furnace. The oxidation temperature was measured by two chromel-alumel thermocouples placed between the furnace wall and mullite reaction tube of the assembly. One of the thermocouples was connected to a Philips controller-recorder and the other to a potentiometer. The controller-recorder was coupled with a mercury relay switch and powerstat allowing

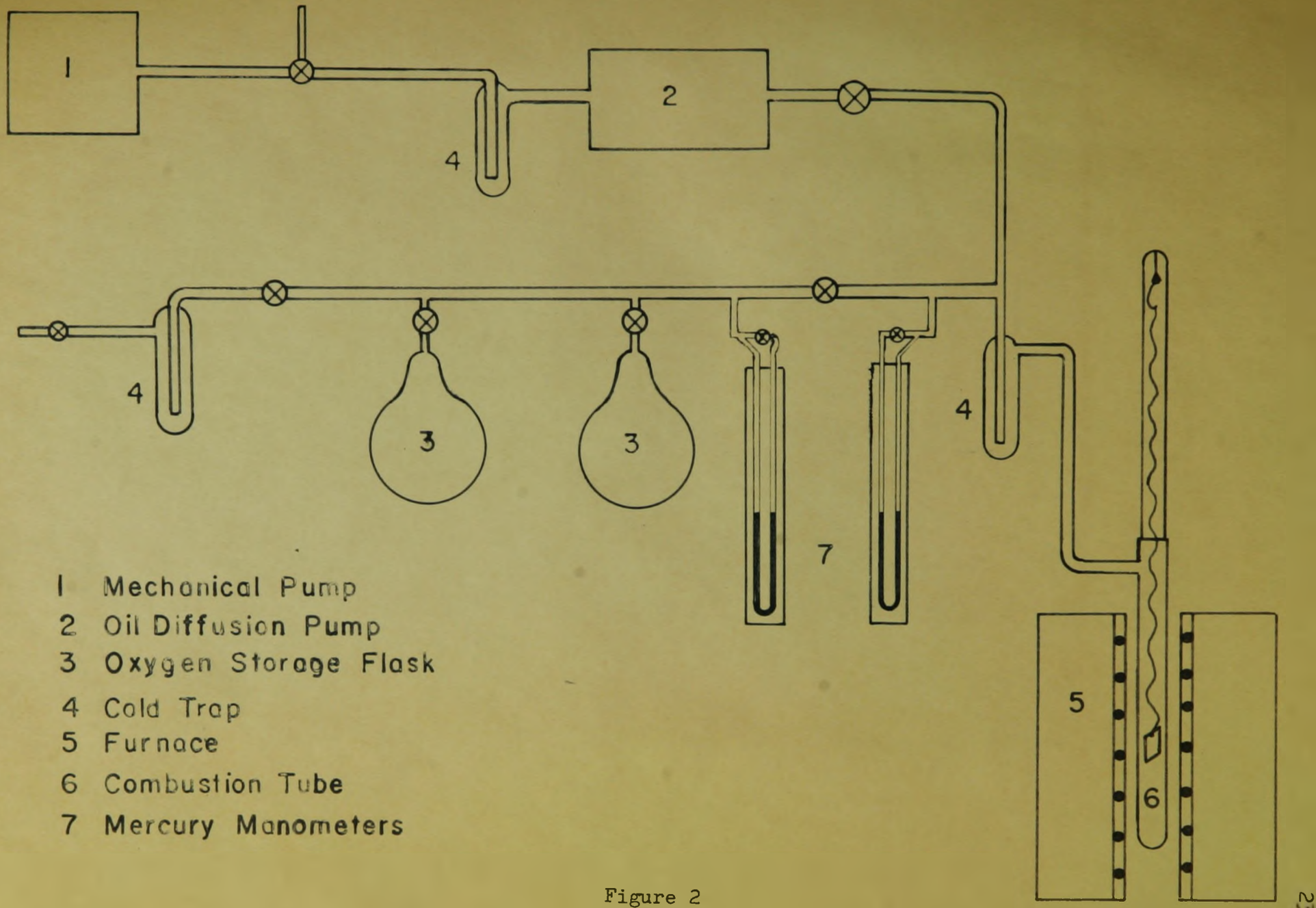

Figure 2

Schematic Diagram of the Oxidation Apparatus

the furnace after cooling in situ. The oxide layer was removed from the specimen and then replaced on the spring balance. The furnace tube was then evacuated to 10^{-6} mm Hg pressure and the furnace heated to 850°C. Oxygen was then admitted to the tube for reoxidation of the specimen. The weight gain was recorded with time. In the second set of experiments, thin specimens 0.254 mm thick, were oxidized at 750 mm Hg pressure at oxygen atmosphere to a weight gain of about 300 atom percent for saturation of the specimen in the alpha phase as taken from the constitutional diagram of the zirconium-oxygen system (45). The furnace was then evacuated and the oxidized specimen annealed for 100 hours for the formation of saturated alpha-solid solution by the diffusion of oxygen from the oxide layer to the metal core. After this annealing process, the specimen was oxidized at 850°C and 750 mm of Hg pressure for growth rate determination.

4.2 Sample Material and Surface Preparation

The zirconium metal prepared by the iodide process was received as 0.04 and 0.125-in gauge sheet. Specimens approximately 3 mm thick and about 10 mm square were prepared by abrasion with silicon carbide papers to a 4/0 fineness for the microhardness tests. For the oxidation kinetics measurements the specimens were about 1 mm thick. Some of the specimens were prepared by chemical etching after polishing on papers. The solution (5 percent HF, 40 percent HNO_3 and the rest water) for polishing the specimen by etching was found to produce a smooth surface.

4.3 Metallographic Mounting and Polishing

A great deal of difficulty was encountered both in mounting and polishing the specimens. During mounting, the oxide tended to break

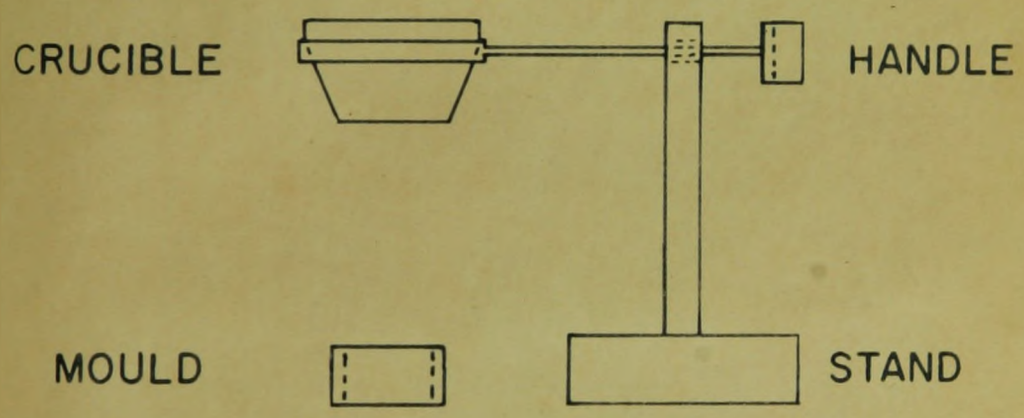

Figure 3

Vacuum Mounting Apparatus

320, 400 and 600 silicon carbide papers with flowing water as lubricant. This was followed by hand polishing on silk cloths using 6, 1 and 1/4-μ diamond paste with lapping oil lubricant. Final polishing was done on polishing wheels using 0.3 and 0.1-μ alumina slurries.

4.3 (c) HARDNESS MEASUREMENTS

Hardness measurements were employed as a measure of oxygen concentration in the metal substrate. Indentation measurements were made adjacent to the metal/oxide surface at a known distance using a Vickers microhardness unit. Five hardness scans were determined for each oxidized specimen and the arithmetical averages taken for the determination. Individual measurements were reproducible within ± 10 percent.

CHAPTER V

EXPERIMENTAL RESULTS

The results of the oxidation tests on weight gain measurements are presented in conjunction with the microhardness determinations and metallographic examinations.

5.1 The Scales

The oxidized specimens produced during this series of experiments for the periods up to 40-50 hours had shiny gray-black scales with white ridges showing on the edges. Metallographic examination of these scales showed that they were dense without any porosity. They adhered strongly to the metal. Detached gray oxide from the metal turned white on heating in air or oxygen. Layering, of the type reported in titanium (28) scales, was not observed in any of the scales on zirconium.

The photomicrographs in figures 4-6 exhibit several features of the scales produced by oxidation at 850°C for different exposure times. As illustrated by the photomicrograph in figure 4, the scale produced upon an exposure of 20 hours is uniform and free of any detectable pores.

The photomicrograph in figure 5 shows an inside gray oxide layer and an outside thin porous layer of oxide formed by oxidation of a specimen at 850°C for 80 hours. The scale is considerably thicker but still uniform. As shown in figure 6, this uniformity vanishes for longer periods of oxidation.

Microhardness examinations were undertaken to establish whether a duplex scale was formed during linear oxidation. The scale developed

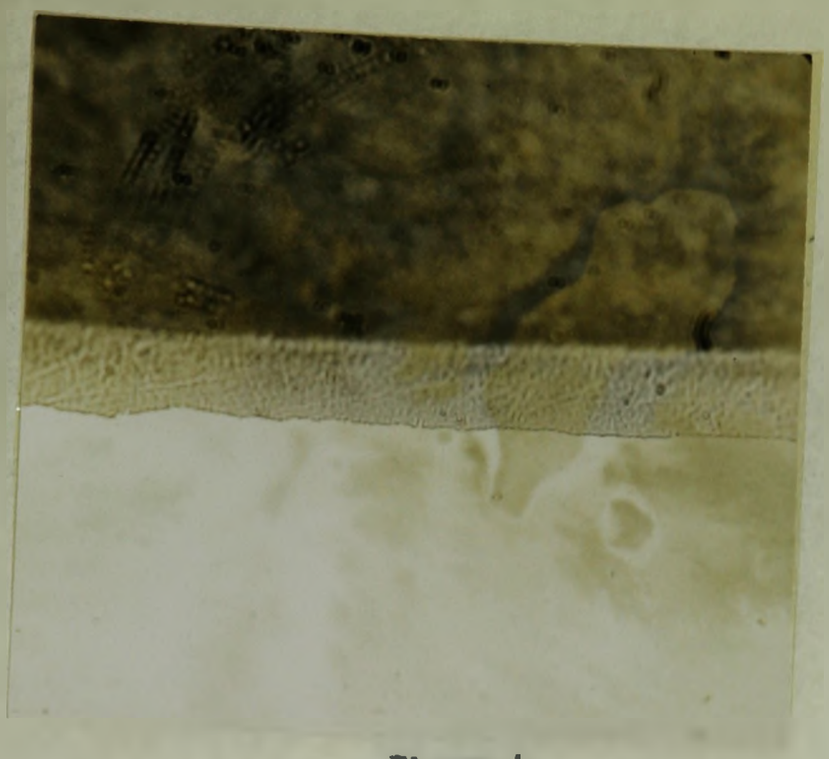

Figure 4

Specimen exposed for 20 hours at 850°C; X 337.5

Figure 5

Specimen oxidized for 80 hours at 850°C; X 337.5

Figure 6

Specimen oxidized for 100 hours at 850°C; X 187.5

Figure 7

Specimen exposed for 60 hours at 850°C; X 120

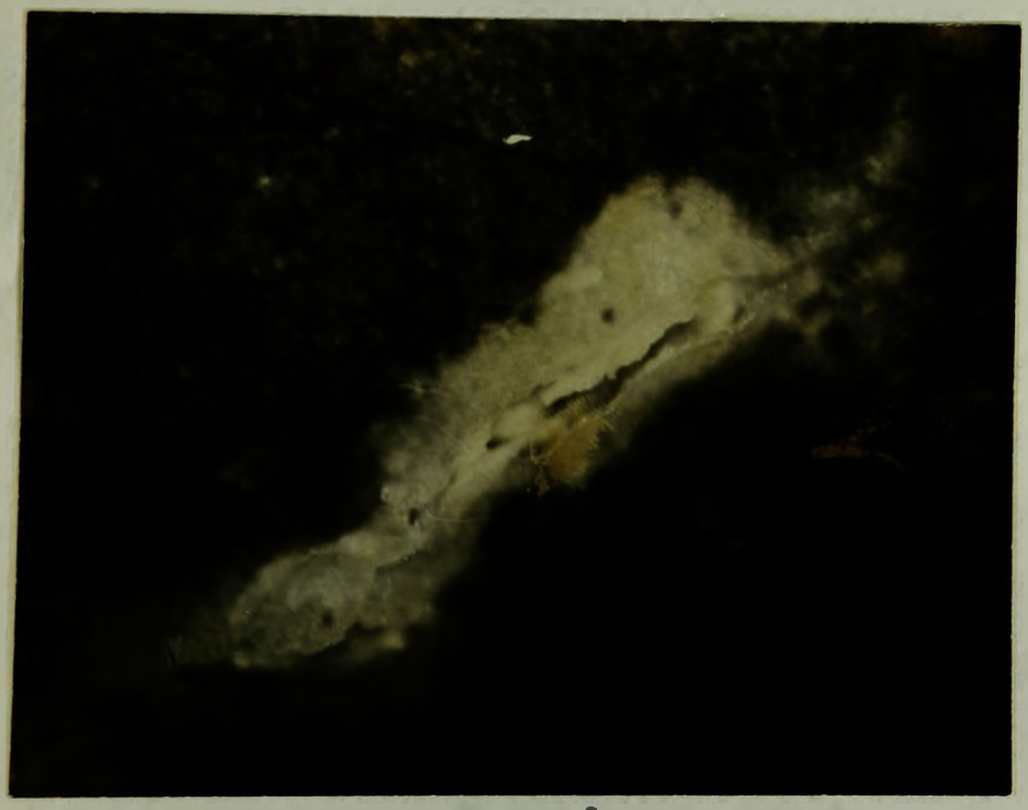

Figure 8

Specimen saturated with oxygen and exposed for 30 hours at 850°C; X 240

during linear oxidation appeared to be composed of an outer porous oxide overlying the remnant gray compact oxide (figure 7-9). The external appearance of the white oxide is shown in figure 7. Its surface exhibits a network of cracks. The original abrasion scratches have persisted because oxidation proceeded by inward migration of oxygen. The breakaway of an oxide section from the surface of specimen (the lower right hand corner of this photomicrograph) has exhibited the underlying compact gray oxide. A number of localized white areas were noticed on the gray oxide before the whole surface became covered with white oxide. Porous oxide growth appeared to be initiated by localized attack associated with crack formation as shown in figure 8.

Some of the specimens with gray oxide were heated in air for a short time to gain additional observations on the characteristics of white oxide formation. It was found that white oxide readily formed at cracks formed in the oxide due to thermal shock upon quenching of oxidized specimens. This characteristic is illustrated by the photomicrograph in figure 10. White oxide formation is also shown in areas derived of thermal cracks. Consequently, the gray oxide scales on several oxidized specimens were examined to find if possible, the approximate grain size of oxide in the scale. For this purpose the oxide scales were etched in hydrofluoric acid and then examined under microscope. Very small surface cracks were found to exist in the oxide which appeared to follow grain boundaries (figure 11). However, it was not possible to dofinitely establish that those cracks followed grain boundaries and that these cracks served as the localized areas for white oxide formation.

5.2 Microhardness Tests

In order to determine the oxygen gradients in the metal, microhardness measurements were made on specimens oxidized at 850°C for exposures of 24, 36, 48, 60, 83 and 100 hours. The results of these experiments are illustrated in figure 12 and figure 13. Figure 12 shows the gradual increase of hardness as oxygen penetrates inwards due to longer oxidation periods. Within experimental accuracy, the concentration of oxygen as a function of distance in the metal is defined by a steady configuration during linear oxidation (figure 13).

5.3 Oxidation Measurements

Measurements were made of the oxidation rates of as-received metal, the metal containing sufficient oxygen for the establishment of a steady state gradient, and the metal saturated with oxygen. The methods for preparing the specimens and measuring these oxidation rates have been presented in the section Oxidation Procedure, 4.1 (d). In figure 14, a photomicrograph is illustrated of a typical surface after preparation by the abrasion method. There are abrasion scratches, which have been shown to remain on the outer surface of compact oxide (figure 7). A photomicrograph is shown in figure 15 of the surface of an oxidized specimen after removal of the oxide by stripping and a subsequent light abrasion. In this case the surface is very irregular.

5.4 Oxidation Rates of the As-Received Metal

In figure 16, results are shown of experiments at 800° and 850°C for long oxidation exposures. Here, the weight gains of zirconium specimens, mg oxygen/cm^2, have been plotted vs time in hours. The oxidation rates continuously decreased for exposures to approximately 60 hours after

Figure 9

The Corner of an Oxidized Specimen. After exposure for 80 hours at 850°C; X 187.

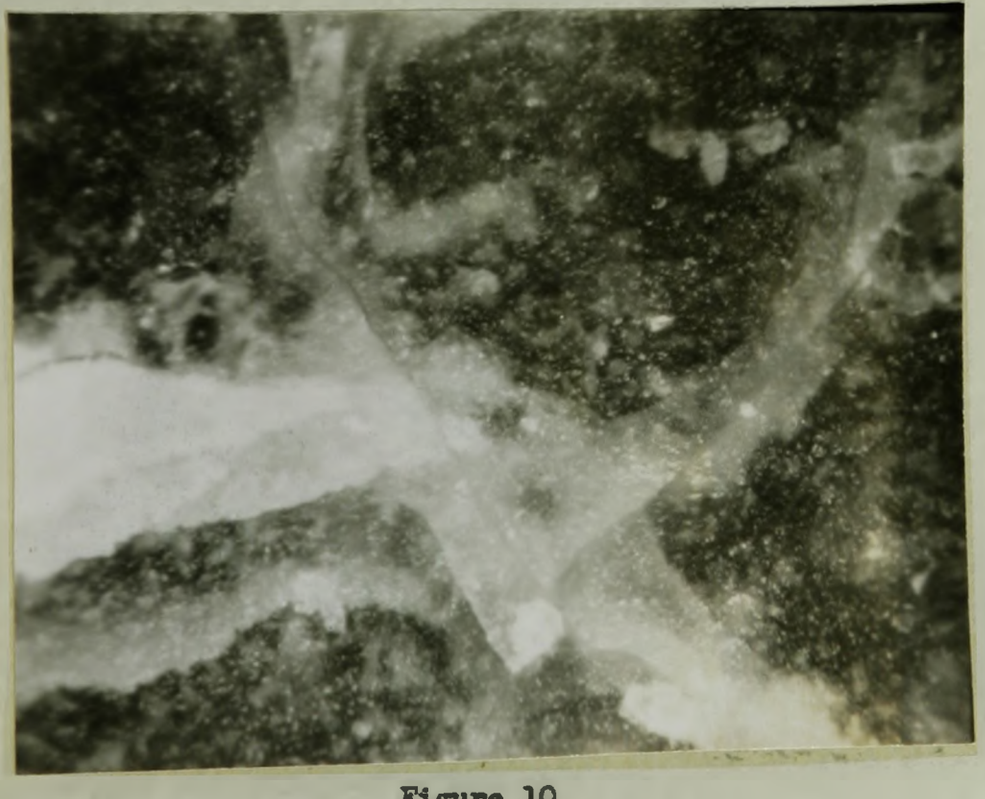

Figure 10

White oxide formed at the cracks in the gray oxide after re-oxidation of specimen in air at 850°C. (Photomicrographs taken under polarized light at magnification of 150 X.)

Figure 11

Cracks in Gray Oxide Surface after etching by HF (X 540). The specimen had been exposed in oxygen for 24 hours at 850°C.

Figure 13

Microhardness determinations of zirconium specimens oxidized for 60, 83, and 100 hours at 850°C and 750 mm Hg pressure.

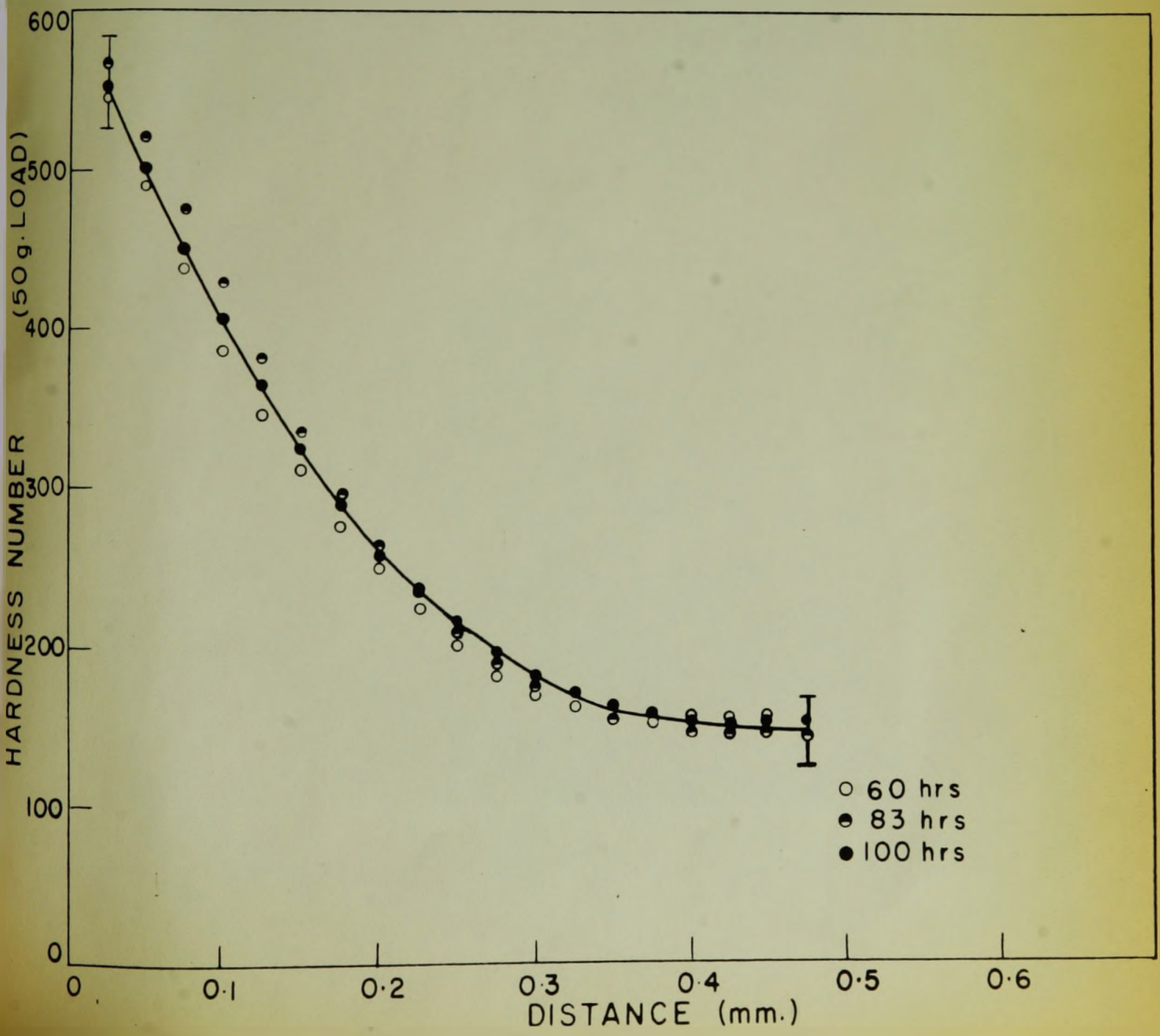

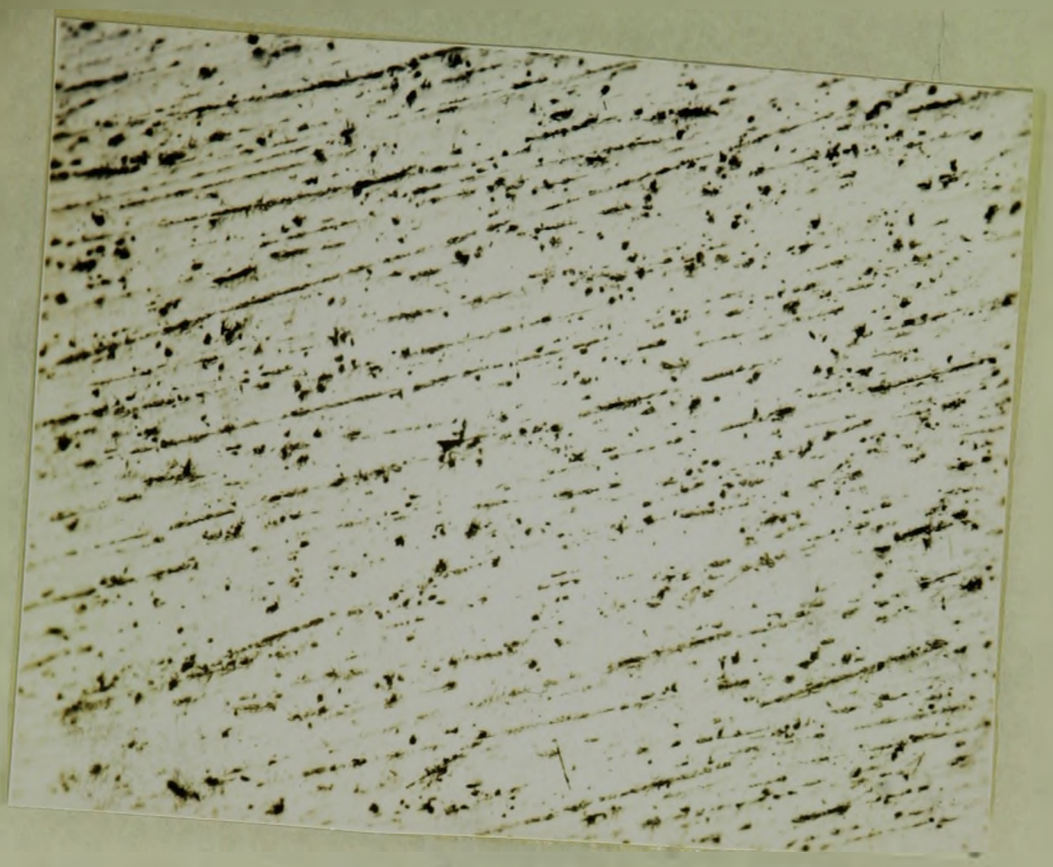

Figure 14

Surface of specimen prepared by abrasion. X240

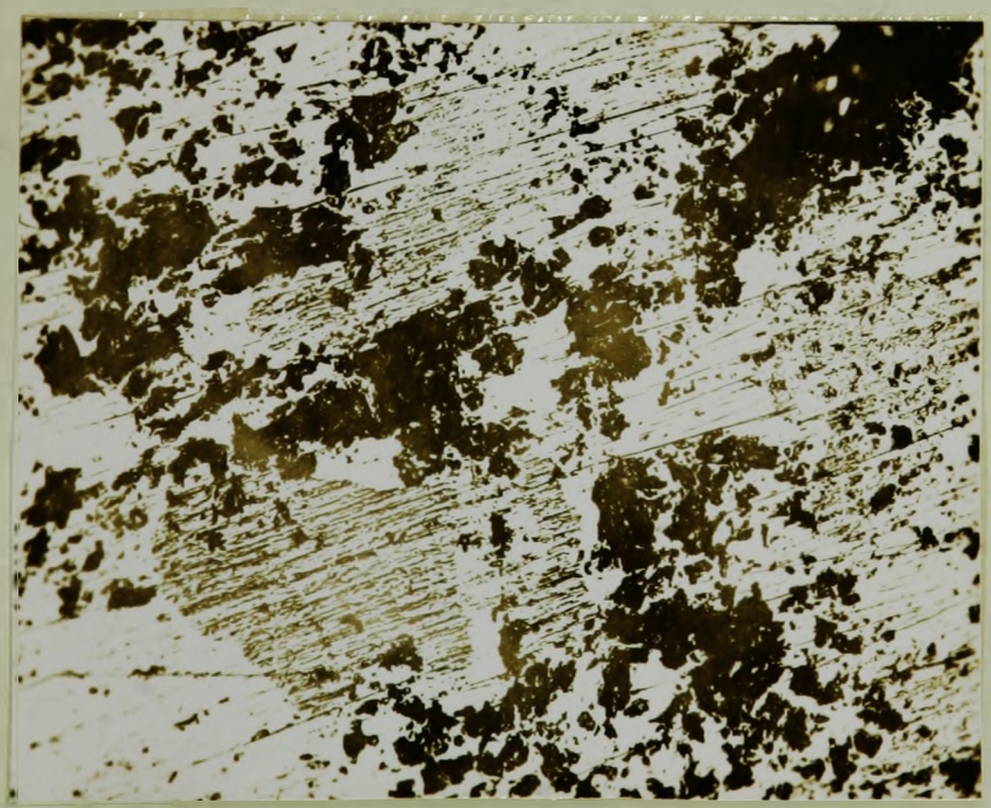

Figure 15

Surface obtained by removal of oxide for re-oxidation. X240

which the specimens oxidized at constant rates. As will be demonstrated, these periods of decreasing and constant rates corresponded to the stages of parabolic and linear oxidation.

5.5 Effect of Oxygen Concentration in Zirconium on Oxidation Rates

To test the possible role of the initial metal oxygen concentration in determining the oxidation kinetics, a series of auxiliary short-time experiments consisting of exposures to 12 hours at 850°C were carried out. As datum experiments, the oxidation kinetics of three as-received specimens containing negligible oxygen contents were determined. The result of these tests are illustrated in figure 17 by parabolic plots, (gm oxygen/cm^2)^2 vs time since, after exposures of approximately 3 hours, the kinetics obeyed a parabolic relationship.

The following experiment was then carried out in duplicate. A specimen was oxidized for 60 hours at 850°C for establishment of the steady configuration of oxygen in metal. After removal from the balance, the scale was chipped from metal surface. The specimen was then lightly abraded on 4/0 silicon carbide paper to remove adhering oxide and replaced in the balance assembly for re-oxidation at 850°C. The oxidation kinetics, figure 18, could still be represented by parabolic plots although their reproducibility was poor. These variations were probably due to non-uniformity of the lightly abraded surfaces (shown in figure 15) from which oxide had been chipped.

Oxidation tests were then carried out on 0.022 cm thick specimens with oxygen contents approaching saturation values. To attain this condition, a specimen was oxidized at 850°C until its weight gain corresponded to 5.0 mg/cm^2 (the saturation value from the phase diagram is

Figure 16

Oxidation of zirconium at 800°C and 850°C in oxygen at 750 mm Hg pressure.

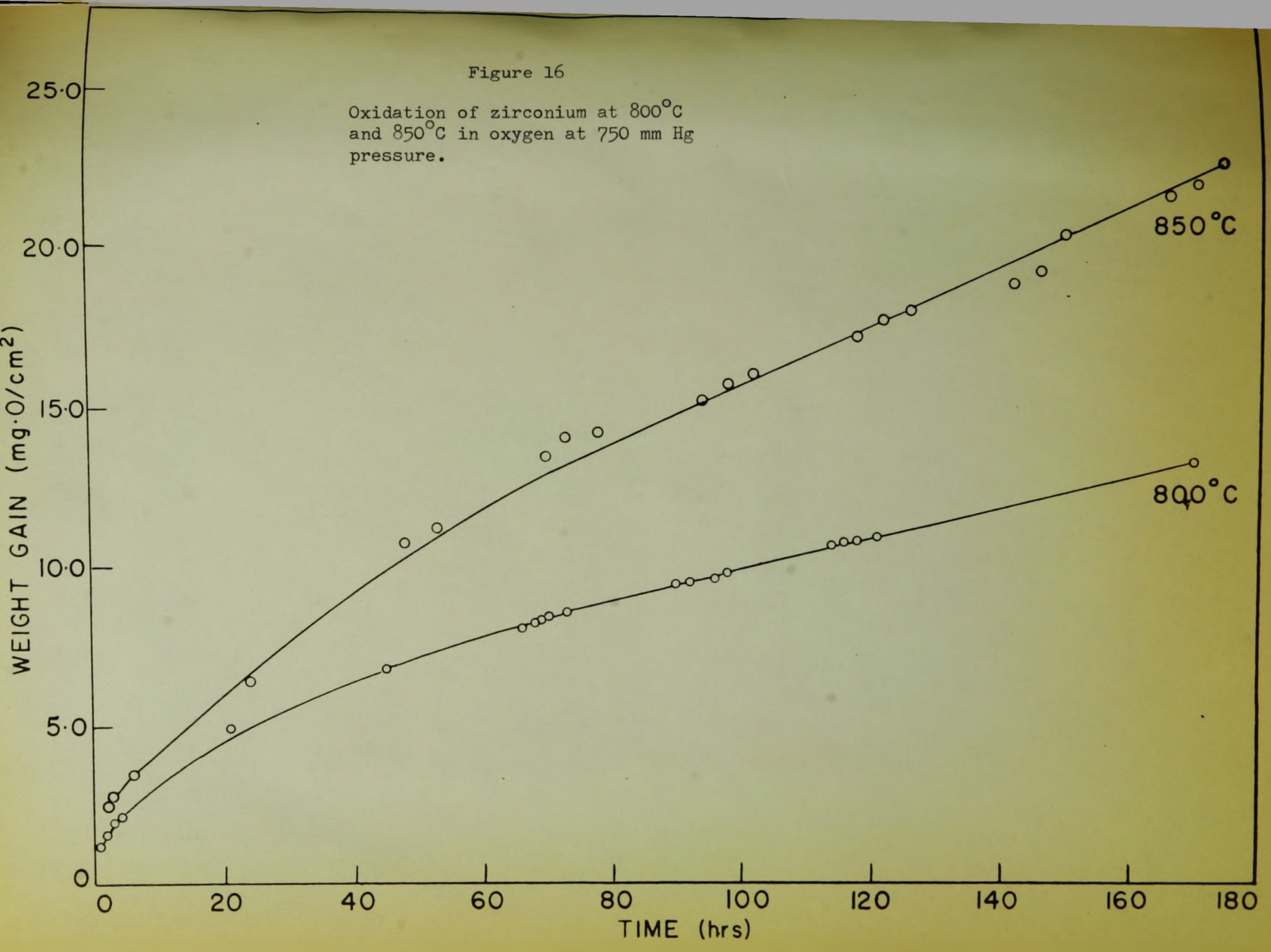

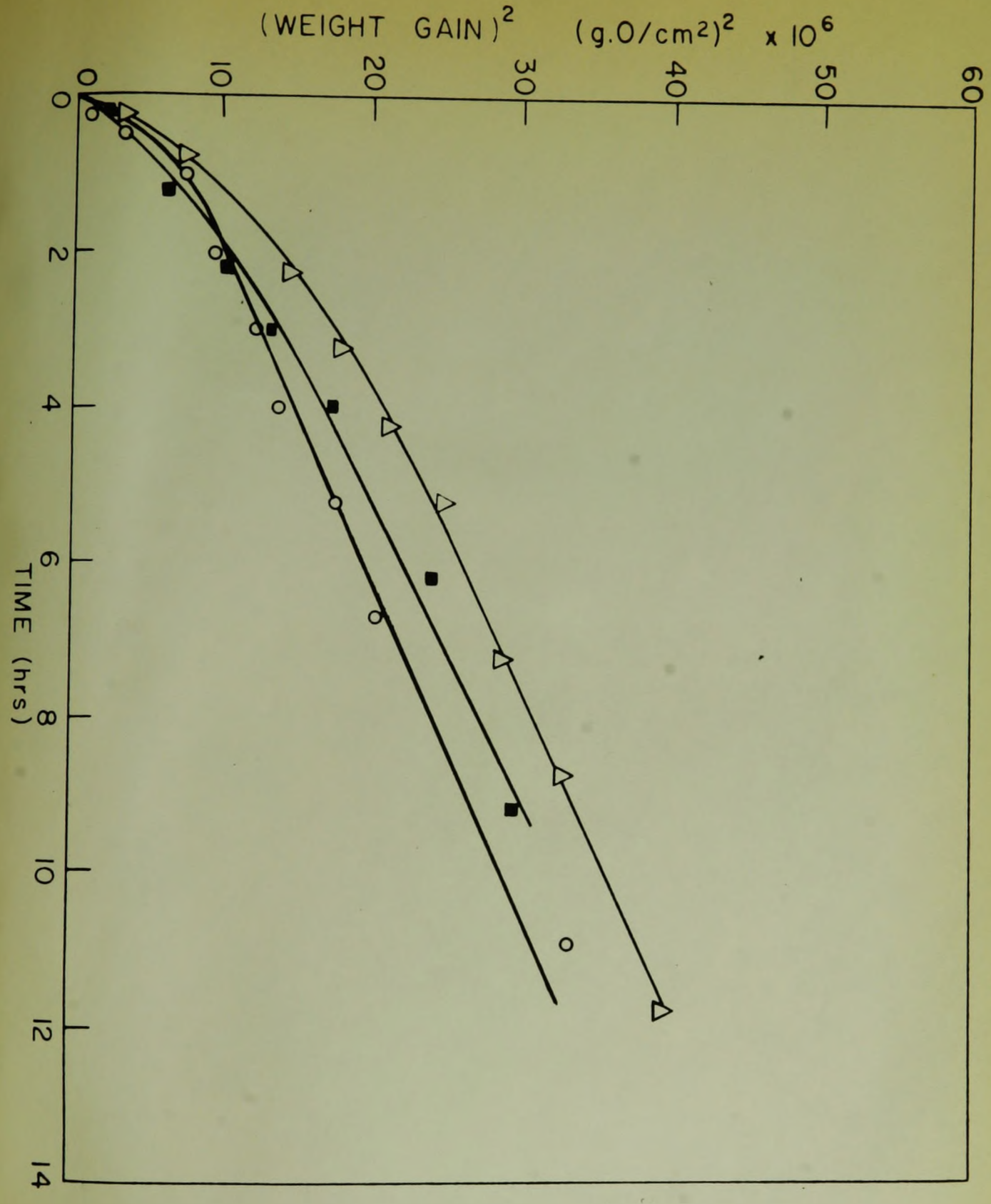

Figure 17

Oxidation of zirconium at 850°C at 750 mm Hg pressure.

Figure 18

Re-oxidation at 850°C in oxygen at
750 mm Hg pressure of zirconium specimen
after removal of compact oxide scale.

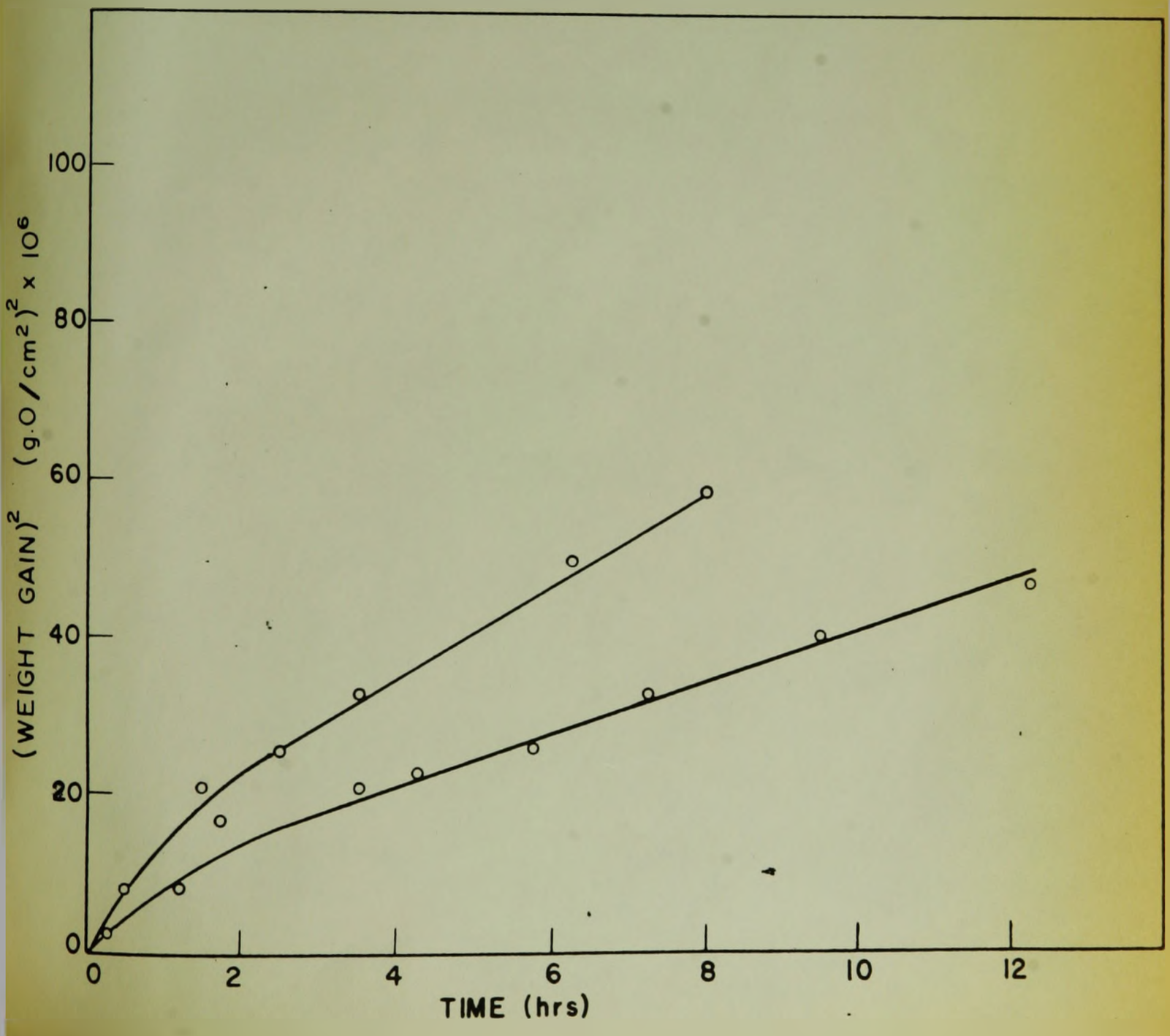

5.1 mg/cm^2) (41). The balance assembly was then subjected to vacuum and specimen annealed for 100 hours so that the oxide would dissolve in the metal. This time was sufficient to redissolve most of the oxide and approximately homogenize the oxygen in the metal. The results for re-oxidation of two such specimens are illustrated by the parabolic plots in figure 19. In agreement with the preceeding tests, the specimens oxidized by parabolic kinetics following brief exposure times.

5.6 Atomic Structure of Scales

The existence of three crystallographic forms: cubic, tetragonal and monoclinic have been reported by different investigators. Both the gray and white oxide structures were examined separately by x-ray analysis. Parameters were calculated from the diffraction lines and then related to the published parameters for different forms of zirconium oxide. Only the monoclinic structure was identified. It was not possible to measure a difference in the parameters between the gray monoclinic and white monoclinic structures.

Figure 19

Oxidation at 850°C in oxygen at 750 mm Hg pressure of zirconium specimen saturated with oxygen.

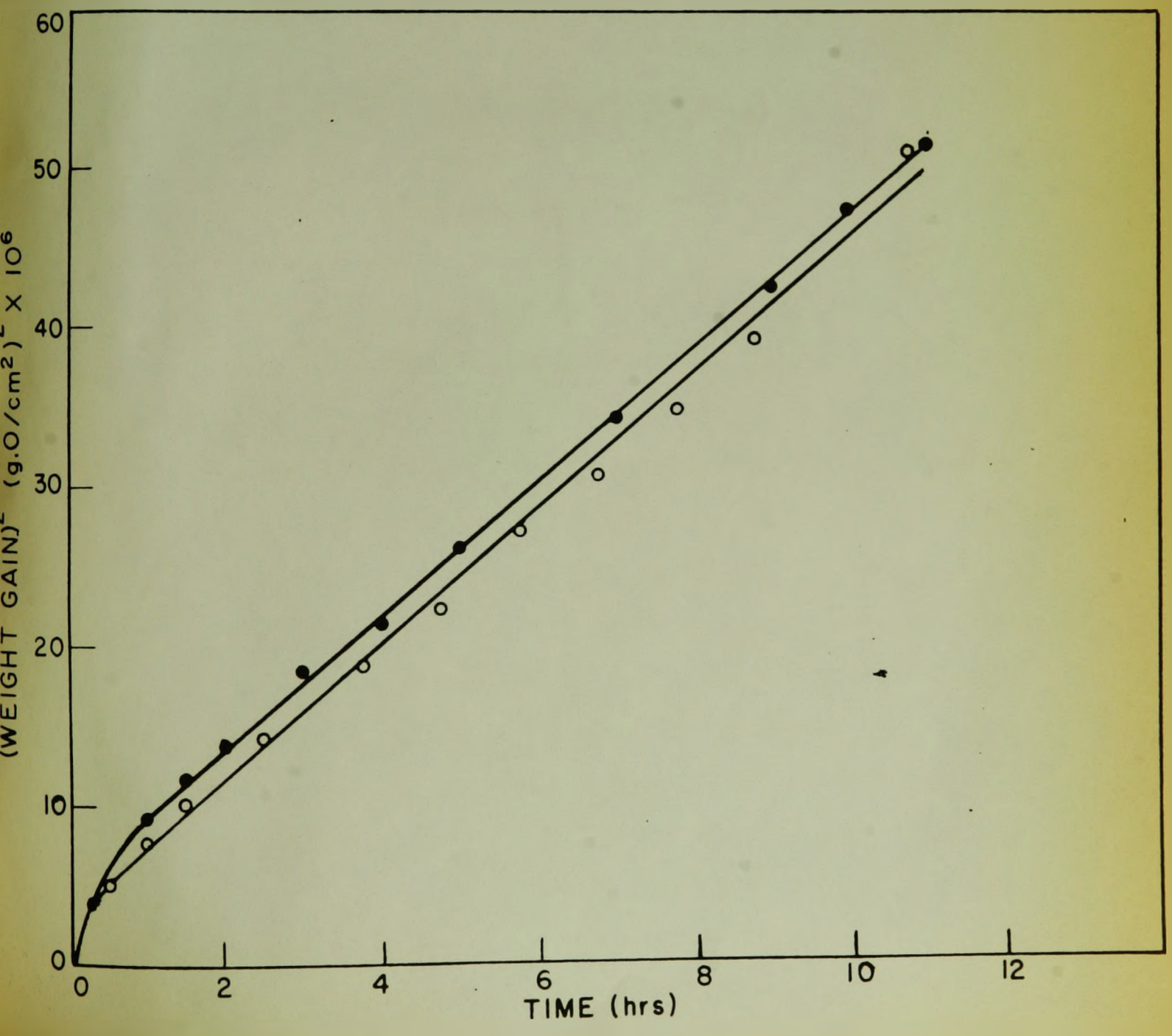

CHAPTER VI

DISCUSSION

In this section, the experimental findings are correlated insofar as possible to show that the growth of a duplex scale, consisting of inner compact and outer porous oxide layer determines the parabolic-linear oxidation kinetics. The influence of the compact layer on the oxidation kinetics after establishment of the "steady gradient" of oxygen in metal is also discussed to demonstrate that the linear kinetics are due to the steady diffusion of oxygen through a compact scale of constant thickness. Also, several oxidation features common to zirconium and titanium are discussed in order to further elucidate behaviour of metals in Periodic Subgroup IVB in oxidizing environments.

The experiments have demonstrated that parabolic oxidation occurs before onset of linear oxidation irrespective of the metallic oxygen contents. This oxidation behaviour was illustrated by the plots in figure 16 for specimens exposed in oxygen for long exposures at 800° and 850°C and the plots of oxidation data for relatively short exposures at 850°C in figure 17 - 19. In table 1, the evaluations are recorded of the parabolic constants at 850°C from the plots in figures 17 - 19 for the as-received metal, for the metal containing sufficient oxygen for establishment of the steady gradient, and for the metal saturated with oxygen. These evaluations are of the same order of magnitude.

One cannot formulate conclusions as to the relative amounts of oxygen consumed by oxide formation and solution in the metal from these

TABLE I

Parabolic Oxidation Constants for Zirconium

Metal	Temperature °C	Parabolic Constant $(g.oxygen)^2/cm^4$-sec
Received metal	800°	2.8×10^{-10}
Received metal	850°	7.5×10^{-10}
		7.2×10^{-10}
		6.4×10^{-10}
Metal with oxygen sufficient to establish gradient before linear oxidation	850°	9.2×10^{-10}
		1.7×10^{-9}
Metal saturated with oxygen	850°	1.2×10^{-9}
		1.2×10^{-9}

evaluations because the oxygen saturated specimens oxidized at the most rapid rate. This effect has also been established by Ostagen and Kofstad (46). For the specimens of their tests, linear oxidation occurred in the time periods reported here for parabolic oxidation. From figure (18), it can be seen that the reporducibility of the results for the weight gain in case of reoxidation were not good. This effect may be due to the surface roughness of the specimens prepared by the removal of oxide scale. The photomicrographs in figures 14 and 15 have shown the extreme roughness of these surfaces compared to those surfaces prepared by abrasion.

The total uptake of oxygen by the metal during oxidation may be evaluated if equation (7) accounts for the amount of dissolved oxygen in the metal during linear oxidation. This amount may then be compared with the total uptake of oxygen during parabolic oxidation. The average values of the ratio (K_L/D_o^I) at 850° and 800°C are 108 and 271 respectively (table II). These values were calculated from the data presented in figures 13 and 16. The consumption of oxygen by the metal is therefore 4.8×10^{-3} and 1.7×10^{-3} gm/cm^2. Since the total uptakes of oxygen before onset of linear oxidation are 1.6×10^{-2} and 1.0×10^{-2} gm/cm^2 at 850° and 800°C, respectively (figure 16), oxygen solution accounts for 30 and 17 percent of the oxygen consumed during parabolic oxidation. One may therefore conclude that oxygen weight-gain kinetics of zirconium at temperatures to 850°C are mainly associated with scale growth.

An evaluation cannot be made of the parabolic oxidation constant in the absence of data for the oxygen diffusion constant and phase boundary compositions for zirconium dioxide. Nevertheless, it is

TABLE II

Evaluations of Linear Oxidation Rate Constants and of Oxygen Diffusion Constants for Zirconium and Titanium and a Comparison of These Values to Those Obtained from Diffusion Penetration Experiments (references in brackets)

Metal	Temperature °C	Exposure Times for Oxygen Gradient Establishment hours	K_L/D	K_L $\frac{g.oxygen}{cm^2\text{-}sec}$	D (oxidation) cm^2/sec	D (diffusion) cm^2/sec
Zr	800		271	1.3×10^{-8}		2.9×10^{-10} (52)
						6.7×10^{-10} (50)
	850	60 - 100	72	2.6×10^{-8}	2.4×10^{-10}	8.7×10^{-10} (52)
		24 - 72	143(47)		1.2×10^{-10}	9.4×10^{-10} (50)
Ti	750	36-48	365(6)	1.9×10^{-8}(1)	3.0×10^{-11}	4.1×10^{-10} (48)
						1.1×10^{-11} (8)
						3×10^{-11} (51)
	850	24-48	144(6)	1.1×10^{-7}(7)	4.6×10^{-10}	1.8×10^{-9} (48)
				1.6×10^{-7}(8)	6.3×10^{-10}	1.2×10^{-10} (8)
						4.1×10^{-10} (51)

possible to test whether steady state diffusion conditions exist in the metal and compact oxide layer during linear oxidation. For this type of oxidation, equation (4) and (15) describe the limiting penetration curve for oxygen in the metal and the conditions for duplex scale formation.

To perform this test for the oxygen gradient in the metal it is assumed that the hardness determinations of the metal are directly proportional to its oxygen concentrations. That such an assumption is reasonable is borne out by hardness measurements of Treco and Roe, Palmer and Open (47, 48) on zirconium and titanium oxygen solid solutions respectively. Accordingly, equation (4) for the concentration gradient of oxygen in the metal during linear oxidation is expressed in the form,

$$\log (H_x - H_o) = \log (H_o^I - H_o) - \left(\frac{K_L}{D_o^I} \log_{10} e\right)_x \qquad (16)$$

where H_x, H_o^I and H_o are the microhardness determinations within the metal substrate at distance x from the metal/oxide interface, at the metal/oxide interface, and at a distance beyond the penetration of the oxygen gradient, respectively.

The microhardness measurements, figure 12, have shown that the oxygen gradient changes during the parabolic growth. The steady state formation of the oxygen gradient during linear oxidation can be seen from the microhardness measurements illustrated in figure 15. These latter determinations and those reported by Wallwork and Jenkins (8) for titanium are plotted according to the above relationship in figure 20. The exponential relationship represents the penetration data only to a good first approximation, perhaps due to the failure of the

Figure 20

Microhardness determinations plotted according to equation (16), $\log (H_x - H_o)$ vs. x, for zirconium and titanium oxidized to range of linear oxidation

Upper curve: hardness gradient in zirconium after exposures of 60, 80 and 100 hours in oxygen at 750 mm. Hg. pressure at 850°C.

Lower curve: hardness gradients in titanium after exposures of 24-48 hours in oxygen at 760 mm. Hg. pressure at 750° and 850°C. Determinations by Wallwork and Jenkins[8].

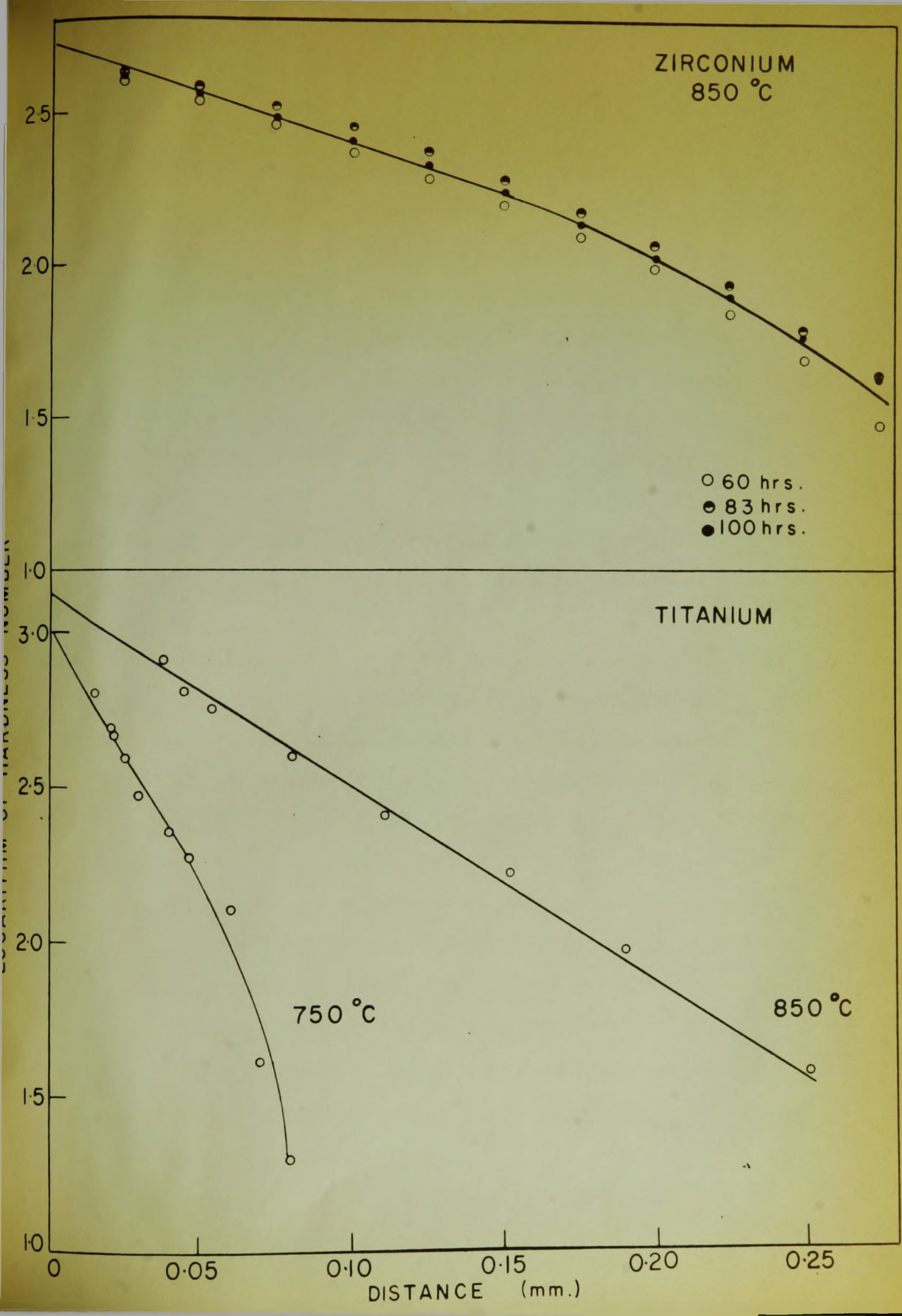
ZIRCONIUM
850 °C
○ 60 hrs.
◒ 83 hrs.
● 100 hrs.
TITANIUM
750 °C
850 °C
2·5
2·0
1·5
1·0
3·0
2·5
2·0
1·5
1·0
0
0·05
0·10
0·15
0·20
0·25
DISTANCE (mm.)

assumption of linearity between concentration and hardness. Nevertheless, the slope of these curves near the interface should give a good estimate of the ratio, K_L/D_o^I, for comparison with independently measured values.

The values of the oxygen diffusion constants calculated from this oxidation data for zirconium and titanium and a comparison of these values with those reported in the literature from diffusion penetration anneal experiments are recorded in table II. For zirconium, an additional determination is also included from an analysis of unpublished oxidation results obtained by Wallwork (49). The comparison lies in all cases within experimental error, thus confirming the essential correctness of that part of the diffusion model which refers to the metal substrate.

The consistency of the linear oxidation kinetics with diffusion conditions of the duplex scale model may be demonstrated by employing equation (15) to calculate the parabolic constant, equation (2), for growth of compact oxide. Since the oxygen uptakes for compact scale growth are 8.3×10^{-3} and 1.12×10^{-2} gm/cm^2 at 800° and 850°C, the values of parabolic constants are 2.3×10^{-10} and 5×10^{-10} gm^2/cm^4/sec, respectively. These values, which are in close agreement with the experimental parabolic constants for the as-received metal (table I), substantiate the consideration that steady state diffusion conditions are satisfied in the inner compact layer during linear oxidation.

While diffusion accounts for the kinetics of oxygen migration during the linear oxidation of zirconium, the primary controlling process providing one of the boundary conditions for diffusion is associated with the mechanical phenomena which maintains a constant thickness of

compact oxide. The metallographic observations do not give information on the mechanism of surface-crack formation. It can be noted from the micrographs of figures 6 - 10 that porous white oxide is formed from compact gray oxide by exfoliation from initiating cracks.

The examinations of the external surfaces of oxide scales produced on specimens by oxidizing for different lengths of time have shown that white oxide was formed on the surface of gray oxide at different points, which in time spread and covered the whole surface of gray oxide with white porous oxide. Compact oxide, which was intimately bonded to the metal, remained gray due to a relatively larger oxygen vacancy concentration. The detached oxide was white because its composition approached that for the oxygen-rich oxide equilibrated with oxygen. In this respect, the parabolic-linear oxidation kinetics of zirconium differ from those for titanium. For this latter metal, the controlling step for linear oxidation appears to be determined by reaction parameters at oxide/metal interface brought into play by a complete breakdown of oxide to a porous scale at a critical thickness (4, 7, 8).

CONCLUSION

From the literature review, theoretical considerations and experimental findings, this thesis can be concluded as follows:

1. The oxidation of zirconium in oxygen at atmospheric pressure follow a parabolic linear growth equation at 800° and 850°C.

2. Irrespective of the oxygen concentration in the metal substrate, parabolic kinetics represent the growth of the initial compact oxide scale while linear kinetics represent the later stages of growth. The transition from parabolic to linear oxidation for zirconium is associated with the formation of a duplex scale consisting of compact and porous oxide layers.

3. The gray compact oxide is formed during parabolic oxidation the inward migration of oxygen to the oxide metal interface. During this stage of the oxidation reaction, oxygen is dissolved in the metal substrate.

4. At a critical thickness of the compact oxide, a steady concentration gradient of oxygen in the metal substrate is established upon onset of linear oxidation kinetics. An exponential solution of the diffusion equation fitted to the concentration profile can be used to evaluate the oxygen diffusion constant in the metal.

5. The oxide formed on the surface of gray oxide during linear growth is white and porous. The structure of both gray and white oxide are monoclinic.

6. The thickness of the compact gray oxide remains constant during linear oxidation by its conversion to white porous oxide. This oxide offered no resistance to the migration of oxygen from gas phase to porous oxide/compact oxide interface.

7. The white porous oxide appeared to form at cracks on the gray oxide surface and then spread by an exfoliating cracking type mechanism. It was impossible to show by chemical etching experiments with hydrofluoric acid whether these cracks occurred at grain boundaries in the compact oxide.

BIBLIOGRAPHY

1. Evans, U.R. The Corrosion and Oxidation of Metals, Edward Arnold Ltd., London (1960).

2. Kubaschewski, O. and Hopkins, B. E. Oxidation of Metals and Alloys, Butterworth, (1953).

3. Wagner, C. Z. Phys. Chem. B 21, (1933).

4. Cabrera, N. and Mott, N.F. Repts. Prog. Phys. 12, 163 (1949).

5. Kofstad, P., Hauffe, K. and Kjollesdal, H. Acta Chem. Scand. 12, 1958, 239.

6. Charles, R.G., Barnartt, S. and Gulbransen, E.A. AIME Trans. 212. (1958), 101.

7. Gulbransen, E.A. and Andrew, K.F. AIME Trans. 209. (1957). 226.

8. Wallwork, G.R. and Jenkins, A.E. J. Electrochem Soc.. 106. (1959), 10.

9. Smeltzer, W.W. and Simnad, M.T. Acta Met.. 5, (1957), 328.

10. Smeltzer, W.W., Haering, R.R. and Kirkaldy, J.S. Acta Met.. 9, (1961), 880.

11. Stringer, J. Acta Met.. 8, (1960) 758.

12. Kofstad, P., Anderson, P.B. and Krudtaa, O.J. J. Less-Common Metals. 3, 1961, 89.

13. Haycock, E.W. J. Electrochem Soc. 106, 1959, 771.

14. Pilling, N.B. and Bedworth, R.E. J. Inst. Metals, 29, 529 (1923).

15. Wagner, C. Z. Phys. Chem.. B 21, (1933), 25.

16. Wagner, C. Atom Movements, A.S.M. (1951), 153.

17. Kubaschewski, O. and Hopkins, B.E. Oxidation of Metals and Alloys, Butterworth, 1953.

18. Fast, J.D. Metallwirtschaft, 17, (1938), 641.

19. Ehrlich, P. Z. Anorg. Chem., 247. (1941), 53

20. Gulbransen, E.A. and Andrew, K.F. Trans AIME, 185. (1949) 741.

21. Alexander, W.A. and Pidgeon, L.M., Canad. J. Res., B 28., (1950), 60.

22. Waber, J.T., Sturdy, G.E. and Wise, E.N. J. Amer. Chem. Soc., 75, (1953), 2269.

23. Jenkins, A.E. J. Inst. Metals. 82, (1953-54), 213.

24. Simnad, M., Spilners, A. and Katz, O. J. Metals. 7, (1955), 68.

25. Jenkins, A.E. J. Inst. Metals. 84, (1955-56), 1.

26. Kinna, W. and Knorr, W. Z. Metallkunde. 47, (1956), 594.

27. Kofstad, P., Hauffe, K. and Kzollesdale, H. Acta Chem. Scand. 12, (1958), 239.

28. Wallwork, G.R. Thesis on Solid Gas Reaction at High Temperatures, (1959), 36-74.

29. Cubiciotti, D. J. Amer. Chem. Soc., 72. (1950), 4138.

30. Cubiciotti, D. J. Amer. Chem. Soc., 73. (1951), 2032.

31. Litton, F.B. Metal Progress. 60. (1951), 83.

32. Treco, R.M. J. Metals. 5. (1953), 284.

33. Hayes, E.T. and Roberson, A.H. Trans. Electrochem. Soc., 96. (1949), 142.

34. Hayes, E.T. and Roberson, A.H. Trans. Electrochem. Soc., 96, (1949), 380.

35. Gulbransen, E.A. and Andrew, K.F. J. of Metals. 1, (1949), 515-741.

36. Phalnikar, C.A. and Baldwin, W.M. Jr., A.S.T.M. Proceedings 43, (1951), 1038.

37. Belle, J. and Mallett, M.W. J. Electrochem. Soc., 101, (1954), 339.

38. Charles, R. G., Barnatt, S. and Gulbransen, E.A. J. of Metals. 9, (1958), 101.

39. Kendall, R.F. A.E.C. Research and Development Report: HW 39 190, Sept., (1955).

40. Cox, B. J. Electrochem. Soc. 108, (1961), 24-27.

41. Wagner, C. Diffusion in Solids, Liquids and Gases. W. Jost. Academic Press, New York, (1952), 71.

42. Tiller, W.A., Jackson, K.A., Rutter, J.W. and Chalmers, B. Acta Met., 1, (1953), 428.

43. Wagner, C. AIME J. Metals. 6, (1954), 154.

44. Smeltzer, W.W. Trans. Can. Inst. Mining and Met., LXIV (1960), 445.

45. Hansen, M. Constitution of Binary Alloys, McGraw-Hill Book Co. Inc., New York, (1958), 1072.

46. Osthagen, K. and Kofstad, P. J. Electrochem. Soc., 109, (1962), 204.

47. Treco, R.M. Zirconium and Zirconium Alloys, Am. Soc. for Metals. (1953), 254.

48. Roe, W.P., Palmer, H.R. and Opie, W.R. Trans. Am. Soc. Metals. 52, (1960), 191.

49. Wallwork, G.R. Private communication.

50. Pemsler, J.P. J. Electrochem. Soc., 105, (1958), 315.

51. Reynolds, J.E., Ogden, H.R. and Jaffe, R.J. Trans. Am. Soc Metals. 49, (1957), 280.

52. Davis, M., Montgomery, K.R. and Standring, J. J. Inst. Metals. 89, (1961), 172.